

The Effect of Noise on Camera Calibration Parameters

Sunil Kopparapu¹ and Peter Corke

¹Automation, CSIRO Manufacturing Science and Technology, P.O. Box 883, Kenmore, Queensland 4069, Australia

Received July 6, 1998; revised May 16, 2001; accepted August 10, 2001

Camera calibration is the estimation of parameters (both intrinsic and extrinsic) associated with a camera being used for imaging. Given the world coordinates of a number of precisely placed points in a 3D space, camera calibration requires the measurement of the 2D projection of those scene points on the image plane. While the coordinates of the points in space can be known precisely, the image coordinates that are determined from the digital image are often inaccurate and hence noisy. In this paper, we look at the statistics of the behavior of the camera calibration parameters, which are important for stereo matching, when the image plane measurements are corrupted by noise. We derive analytically the behavior of the camera calibration matrix under noisy conditions and further show that the elements of the camera calibration matrix have a Gaussian distribution if the noise introduced into the measurement system is Gaussian. Under certain approximations we derive relationships between the camera calibration parameters and the noisy camera calibration matrix and compare it with Monte Carlo simulations. © 2001 Elsevier Science (USA)

1. INTRODUCTION

A camera performs a projective perspective transformation of 3D world points to the 2D image plane. Camera calibration is the process of estimating the parameters of this transformation—the pose of the camera with respect to the scene (extrinsic camera parameters) and also focal length, pixel scale, and image center (intrinsic camera parameters). Camera calibration is important for many computer vision applications such as stereo matching [1, 2] or 3D reconstruction [3].

Camera calibration is a “classical” problem in computer vision and photogrammetry. Various camera models and schemes have been proposed in literature, for example, [4–8] to cite a few. The common approach is to introduce into the scene a calibration device that

¹ Current address: Cognitive Systems Research Laboratory, Tata Infotech Limited, Navi Mumbai 400 705, India.



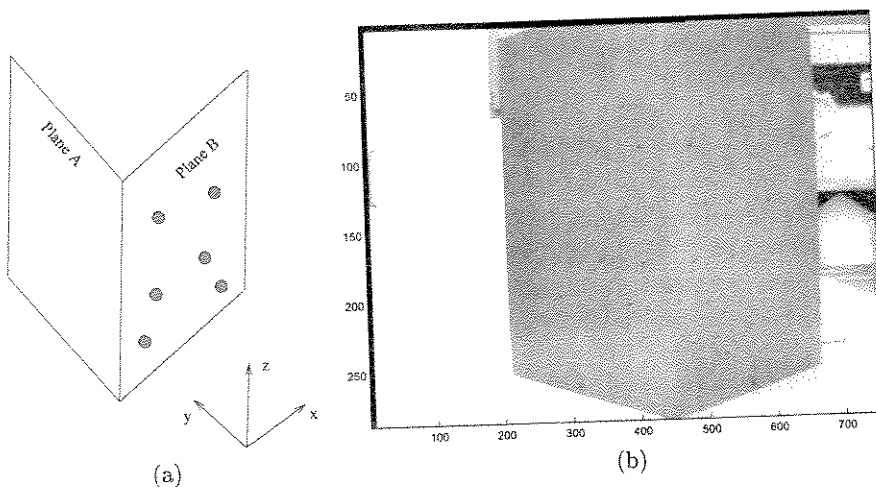


FIG. 1. (a) The precision structure used for calibration of the camera and (b) the actual calibration wedge with precisely marked points used in the experiments.

has a number of points whose relative 3D disposition is accurately known. From the corresponding 2D projections the calibration parameters can be derived using least-squares [9], minimization [10], or gradient [11] techniques. In recent years researchers have shown the feasibility of performing relative calibration between cameras using natural scene points, rather than a special purpose calibration sources [12–14].

In our work we are concerned with the classical single-camera problem of estimating both the intrinsic and the extrinsic parameters [15]. Determining the parameters associated with the camera is a straightforward exercise when the measurements of the 3D points in the scene and the corresponding image points in the 2D image as seen by the camera are accurate. The points in 3D space can be precisely placed—we use a calibration target (Fig. 1) shaped like a wedge on which a number of small calibration marks have been machined. The coordinates of each mark has been measured by a coordinate measuring machine. The problem we investigate in this paper is the effect of small errors in estimating the centroid of the projection of the calibration marks. The point correspondence problem is solved by manually picking the points in the image and then applying some image processing techniques to achieve subpixel accuracy. The errors, although small, have a significant effect on the estimated camera parameters.

In this paper, we assume that the camera calibration parameters are determined using an external calibrated reference source, for example, Fig. 1. We then perform a number of numerical experiments (Monte Carlo simulations) to determine the effect of noise on the camera calibration parameters. This analysis, we think, gives a field engineer an idea of what error in measurements of the points can be tolerated depending on the application, which determines the required accuracy of the mapping between the 3D scene and the 2D image. One can appreciate the significance of such an analysis when one observes that a rotational error of 1° about the optical axis can cause epipolar lines that are vertically aligned on one side of the image to be vertically shifted by more than 10 pixels at the other (using our particular camera and lens configuration) and this, for most applications, is unacceptable. We also determine analytically the bounds on the camera calibration matrix as a function of the bounds on the errors in measurement. In addition we show that (with reasonable approximation), when the error in measurement is Gaussian, so are the elements of the

camera calibration matrix, though with a different variance. To the best of our knowledge, there has been no study of such an analysis in the literature, the closest work being robust estimations of camera location from noisy data having outliers [16] and sensitivity of camera calibration [17, 18]. In [17] while the emphasis is on demonstrating new solutions for estimating the 3D camera location and pose, Kumar and Hanson do devote a section to sensitivity analysis where they study the effect of incorrect estimation of focal length on pose estimation and the incorrect estimation of the image center on the pose estimation separately. They conclude that (i) incorrect measurement of focal length affects the translational parameter component parallel to the optical axis and does not have much effect on the other translational and rotation parameters, and (ii) incorrect measurement of image center has no significant effect on the translational parameters; however, the error in the rotation parameters is linearly related to the error in the estimation of image center. In [18] a study of the sensitivity of the camera's intrinsic parameters on the accuracy of measurement is carried out; in essence they study the error in the *real* image point and the predicted image point, which is obtained by transforming the 3D image point into a 2D plane. Unlike [18] we assume that this error is Gaussian and show its effect on different camera calibration parameters, and unlike [17] we assume that the intrinsic parameters like image center is *not* known a priori but is determined as part of the camera calibration process. In fact we show in this paper the effect of measurement noise on the estimation of the image center also.

The organization of the paper is as follows: in Section 2 we introduce the problem of camera calibration. In Section 3 we derive bounds on the elements of the camera calibration matrix and also show that the camera calibration matrix elements have Gaussian distribution when the measurement errors are Gaussian. In Section 4 we show the effect of the noisy camera calibration matrix on the camera calibration parameters, both intrinsic and extrinsic parameters. We use Monte Carlo simulation methods in Section 5 to show the effect of noise on the camera calibration parameters and compare the experimental results with the developed theory (Section 4), and finally in Section 6 we discuss the results and conclude.

2. CAMERA CALIBRATION

The relationship between the world camera coordinates $[x \ y \ z]$ and the image coordinates $[u = U/W \ v = V/W]$ can be written in the homogeneous coordinate system as

$$\begin{bmatrix} U \\ V \\ W \end{bmatrix} = \underbrace{\begin{bmatrix} C_{11} & C_{12} & C_{13} & C_{14} \\ C_{21} & C_{22} & C_{23} & C_{24} \\ C_{31} & C_{32} & C_{33} & C_{34} \end{bmatrix}}_C \begin{bmatrix} x \\ y \\ z \\ 1 \end{bmatrix}, \quad (1)$$

where C is the *camera calibration matrix*, a 3×4 homogeneous transform that performs scaling, translation, and perspective. C represents the relationship between 3D world coordinates and their corresponding 2D image coordinates as seen by the computer.

Using the knowledge of n world coordinates of the points (given) and their corresponding image coordinates (derived from the image) one can rewrite (1) as

$$\begin{bmatrix} x_1 & y_1 & z_1 & 1 & 0 & 0 & 0 & -u_1 x_1 & -u_1 y_1 & -u_1 z_1 \\ 0 & 0 & 0 & 0 & x_1 & y_1 & z_1 & 1 & -v_1 x_1 & -v_1 y_1 & -v_1 z_1 \\ \vdots & & & & & & & & & & \\ x_n & y_n & z_n & 1 & 0 & 0 & 0 & -u_n x_n & -u_n y_n & -u_n z_n \\ 0 & 0 & 0 & 0 & x_n & y_n & z_n & 1 & -v_n x_n & -v_n y_n & -v_n z_n \end{bmatrix} \begin{bmatrix} C_{11} \\ C_{12} \\ \vdots \\ C_{33} \end{bmatrix} = \begin{bmatrix} u_1 \\ v_1 \\ \vdots \\ u_n \\ v_n \end{bmatrix}, \quad (2)$$

Without any loss of generality we assume $C_{34} = 1$, and estimate the camera calibration matrix \mathbf{C} using the least-squares method, provided we have at least $n = 6$ points that are not coplanar [19].

The most straightforward way of determining the camera calibration parameters is to precisely position a number of points, namely $\{(x_i, y_i, z_i)\}_{i=1}^n$, in 3D space. This scene is imaged using the camera that is to be calibrated and the positions of these corresponding points in the image, namely, $\{(u_i, v_i)\}_{i=1}^n$ are measured. Using $\{(x_i, y_i, z_i, u_i, v_i)\}_{i=1}^n$ we can determine the lumped camera calibration matrix \mathbf{C} . The camera calibration matrix \mathbf{C} can then be decomposed (see Appendix A) into parameters associated with the camera [20]. The decomposed parameters can be categorized as intrinsic and extrinsic camera parameters. While scaling (α_x and α_y) and principal point or image center (u_o, v_o) compose the intrinsic parameters, the orientation (roll, pitch, yaw) and the camera translation (in the x , y , and z directions) make up the extrinsic parameters. We first show how the error in measurement of (u, v) affects the camera calibration matrix \mathbf{C} . Initially we derive bounds on the camera calibration matrix, which depends on the measurement error bounds, and later show that the distribution of the error in the camera calibration matrix is Gaussian provided the error made in measurement has a Gaussian distribution. In the later part of the paper, we derive relationships between the camera calibration parameters (obtained by decomposing \mathbf{C}) and the error in the camera calibration matrix ($\delta\mathbf{C}$) and later compare it experimentally.

3. CAMERA CALIBRATION MATRIX ERROR BOUNDS

The camera calibration matrix \mathbf{C} can be determined by solving (2) using the least-squares estimate, provided there is no error in the measured points $\{(u_i, v_i)\}$. Unfortunately more often than not there is error in the measure values of $\{(u_i, v_i)\}$, so it is important to first show how the camera calibration matrix \mathbf{C} is affected by the error in measurement; to do this we decouple the matrix equation (2) as

$$[(A_1)_{2n \times 8} \mid (A_2)_{2n \times 3}]_{2n \times 11} \begin{bmatrix} (C_1)_{8 \times 1} \\ (C_2)_{3 \times 1} \end{bmatrix}_{11 \times 1} = \begin{bmatrix} u_1 \\ v_1 \\ \vdots \\ u_n \\ v_n \end{bmatrix}_{2n \times 1}$$

or

$$A_1 C_1 + A_2 C_2 = B, \quad (3)$$

where

$$A_1 = \begin{bmatrix} x_1 & y_1 & z_1 & 1 & 0 & 0 & 0 & 0 \\ 0 & 0 & 0 & 0 & x_1 & y_1 & z_1 & 1 \\ \vdots & & & & & & & \\ x_n & y_n & z_n & n & 0 & 0 & 0 & 0 \\ 0 & 0 & 0 & 0 & x_n & y_n & z_n & n \end{bmatrix}_{2n \times 8} \quad A_2 = \begin{bmatrix} -u_1 x_1 & -u_1 y_1 & -u_1 z_1 \\ -v_1 x_1 & -v_1 y_1 & -v_1 z_1 \\ \vdots & & \\ -u_n x_n & -u_n y_n & -u_n z_n \\ -v_n x_n & -v_n y_n & -v_n z_n \end{bmatrix}_{2n \times 3}$$

$$C_1 = \begin{bmatrix} C_{11} \\ C_{12} \\ \vdots \\ C_{24} \end{bmatrix}_{8 \times 1}, \quad C_2 = \begin{bmatrix} C_{13} \\ C_{23} \\ C_{33} \end{bmatrix}_{3 \times 1}, \quad B = \begin{bmatrix} u_1 \\ v_1 \\ \vdots \\ u_n \\ v_n \end{bmatrix}_{2n \times 1}.$$

Observe that the error in image point measurement occurs in A_2 and B . If δA_2 and δB are the errors introduced because of measurement, this results in an error in the camera calibration matrix, which we denote by δC_1 and δC_2 . Then we have

$$A_1(C_1 + \delta C_1) + (A_2 + \delta A_2)(C_2 + \delta C_2) = B + \delta B.$$

Using (3), we have

$$A_1\delta C_1 + A_2\delta C_2 + \delta A_2 C_2 + \delta A_2 \delta C_2 = \delta B.$$

Neglecting second- and higher-order term, $\delta A_2 \delta C_2$ and observing that $A_1\delta C_1 + A_2\delta C_2 = A\delta C$ we have

$$\begin{aligned} A\delta C &= \delta B - \delta A_2 C_2 \\ \delta C &= A^\dagger(\delta B - \delta A_2 C_2). \end{aligned}$$

Now, if the error in measurements δB and δA_2 are bounded as

$$\begin{aligned} A_2^l &\leq \delta A_2 \leq A_2^h \\ B^l &\leq \delta B \leq B^h, \end{aligned}$$

then we can place bounds on δC as

$$C^l \leq \delta C \leq C^h, \tag{4}$$

where

$$\begin{aligned} C^l &= A^\dagger(B^l - A_2^h C_2) \\ C^h &= A^\dagger(B^h - A_2^l C_2), \end{aligned}$$

where A^\dagger is the pseudo inverse of A and is assumed to exist. These bounds (4) on the camera calibration parameters are useful because they suggest the possible accuracy with which B and C_2 must be measured to keep the camera calibration matrix parameters within the required bounds.

It is found experimentally that the error introduced in measuring the image positions has a Gaussian distribution (see Fig. 5). Now, we show how the statistics of the camera calibration matrix (C) elements are affected when the error in measurement has a Gaussian distribution. We know that the error in the camera calibration matrix δC and the error in the measurements δB , δA_2 are related by

$$\delta C = A^\dagger(\delta B - \delta A_2 C_2).$$

Let δB and δA_2 be independent and Gaussian with zero mean and variance σ_b^2 and $\sigma_{a_2}^2$ respectively, then

$$f_{\delta B}(\delta b) = \frac{1}{\sqrt{2\pi\sigma_b^2}} \exp^{-\left\{\frac{(\delta b - \mu_b)^T}{\sigma_b^2}\right\}}$$

and

$$f_{\delta A_2}(\delta a_2) = \frac{1}{\sqrt{2\pi\sigma_{a_2}^2}} \exp^{-\left\{\frac{(\delta a_2 - \mu_{a_2})^T}{\sigma_{a_2}^2}\right\}},$$

then we can show (see Appendix B) that the probability density function (pdf) of δC is

$$f_{\delta C}(\delta C) = \frac{1}{\sqrt{2\pi(AA^T)^{-1}(\sigma_{\delta b}^2 + CC^T\sigma_{\delta a_2}^2)}} \exp^{-\left(\frac{\delta C^T(\delta b - \mu_b)^T + CC^T\delta a_2^T}{2\pi(AA^T)^{-1}(\sigma_{\delta b}^2 + CC^T\sigma_{\delta a_2}^2)}\right)}, \quad (5)$$

meaning that the error in the camera calibration matrix elements due to error in measurements has Gaussian distribution with mean 0 and variance $(AA^T)^{-1}(\sigma_{\delta b}^2 + CC^T\sigma_{\delta a_2}^2)$. This shows that the variance of the error in the camera calibration matrix is directly dependent on the variance of the error made in measurement.

Although we have determined the error bounds on the camera calibration matrix elements as affected by the errors made in measuring the image points, we have not shown how the error actually affects the camera calibration parameters (intrinsic and extrinsic). In the next section we show analytically the effect of the error in the camera calibration matrix on the camera calibration parameters (image center, scale, translation, and orientation).

4. EFFECT OF NOISE (δC) ON CAMERA CALIBRATION PARAMETERS

It is important to know the effect that noise in the camera calibration matrix (δC) has on the camera calibration parameters, because finally one would like to know how the parameters that map the 3D scene into a 2D image are affected. Ganapathy [20] (Appendix A) has shown the relation between the camera calibration matrix C and the various camera calibration parameters. If C is the camera calibration matrix (1), then the various parameters can be written in terms of C as:

- Intrinsic parameters
 - Image center

$$\begin{aligned} u_o &= \frac{\sum_{k=1}^3 C_{1k} C_{3k}}{\sum_{l=1}^3 C_{3l}^2} \\ v_o &= \frac{\sum_{k=1}^3 C_{2k} C_{3k}}{\sum_{l=1}^3 C_{3l}^2} \end{aligned} \quad (6)$$

—Scaling factor

$$\begin{aligned}\alpha_x &= \sqrt{\frac{\sum_{k=1}^3 C_{1k}^2}{\sum_{l=1}^3 C_{3l}^2} - u_o^2} \\ \alpha_y &= \sqrt{\frac{\sum_{k=1}^3 C_{2k}^2}{\sum_{l=1}^3 C_{3l}^2} - v_o^2}\end{aligned}\quad (7)$$

• Extrinsic parameters

—Translation

$$\begin{aligned}t_x &= \frac{\frac{C_{1x}}{\sum_{l=1}^3 C_{3l}^2} - u_o \frac{C_{34}}{\sum_{l=1}^3 C_{3l}^2}}{\alpha_x} \\ t_y &= \frac{\frac{C_{2x}}{\sum_{l=1}^3 C_{3l}^2} - v_o \frac{C_{34}}{\sum_{l=1}^3 C_{3l}^2}}{\alpha_y} \\ t_z &= \frac{C_{34}}{\sum_{l=1}^3 C_{3l}^2}\end{aligned}\quad (8)$$

—Orientation. The roll (ϕ), pitch (θ), and vergence (ξ), see Fig. 2, are related to the rotation matrix

$$\mathbf{R} = \begin{bmatrix} R_{11} & R_{12} & R_{13} \\ R_{21} & R_{22} & R_{23} \\ R_{31} & R_{32} & R_{33} \end{bmatrix} = \text{Rot}_Y(\xi) \text{Rot}_X(\theta) \text{Rot}_Z(\phi)$$

as

$$\begin{aligned}\phi &= \tan^{-1} \left(\frac{R_{21}}{R_{11}} \right) \\ \theta &= \tan^{-1} \left(\frac{-R_{31}}{\cos \phi R_{11} + \sin \phi R_{21}} \right) \\ \xi &= \tan^{-1} \left(\frac{\sin \phi R_{13} - \cos \phi R_{23}}{\cos \phi R_{22} + \sin \phi R_{12}} \right).\end{aligned}\quad (9)$$

and the elements of the \mathbf{R} are related to the camera calibration matrix \mathbf{C} by

$$\begin{aligned}R_{1i} &= \frac{\frac{C_{1i}}{\sum_{l=1}^3 C_{3l}^2} - u_o \frac{C_{34}}{\sum_{l=1}^3 C_{3l}^2}}{\alpha_x} \\ R_{2i} &= \frac{\frac{C_{2i}}{\sum_{l=1}^3 C_{3l}^2} - v_o \frac{C_{34}}{\sum_{l=1}^3 C_{3l}^2}}{\alpha_y} \\ R_{3i} &= \frac{C_{3i}}{\sum_{l=1}^3 C_{3l}^2} \quad \text{for } i = 1, 2, 3.\end{aligned}\quad (10)$$

4.1. Effect of Noise (δC) on Image Center (u_o, v_o)

Let $\delta \mathbf{C}$ be the error associated with the camera calibration matrix due to the error in measurements. We know that the image center, (u_o, v_o) can be estimated from \mathbf{C} by (6). Now, if $\delta \mathbf{C}$ represents the error component in the camera calibration matrix, then the image center with an erroneous camera calibration matrix $\mathbf{C} + \delta \mathbf{C}$ can be estimated as

$$\begin{aligned} u_o + \delta u_o &= \frac{\sum_{k=1}^3 (C_{1k} + \delta C)(C_{3k} + \delta C)}{\sum_{l=1}^3 (C_{3l} + \delta C)^2} \\ v_o + \delta v_o &= \frac{\sum_{k=1}^3 (C_{2k} + \delta C)(C_{3k} + \delta C)}{\sum_{l=1}^3 (C_{3l} + \delta C)^2}. \end{aligned} \quad (11)$$

Now, we concentrate on one component (u_o) of the image center because the other component (v_o) follows in similar fashion. From (6) and (11) we can write

$$\delta u_o = \frac{\sum_{k=1}^3 (C_{1k} + \delta C)(C_{3k} + \delta C)}{\sum_{l=1}^3 (C_{3l} + \delta C)^2} - \frac{\sum_{k=1}^3 C_{1k} C_{3k}}{\sum_{l=1}^3 C_{3l}^2}. \quad (12)$$

We can rewrite (12) as

$$\delta u_o = \frac{A^{u_o} + \delta A^{u_o}}{B^{u_o} + \delta B^{u_o}} - \frac{A^{u_o}}{B^{u_o}}, \quad (13)$$

where

$$\begin{aligned} A^{u_o} &= \sum_{k=1}^3 C_{1k} C_{3k} \\ B^{u_o} &= \sum_{l=1}^3 C_{3l}^2 \\ \delta A^{u_o} &= \delta C \sum_{k=1}^3 (C_{1k} + C_{3k}) + 3\delta C^2 \\ \delta B^{u_o} &= 2\delta C \sum_{l=1}^3 C_{3l}^2 + 3\delta C^2. \end{aligned}$$

Now, (13) can be written as

$$\delta u_o = \frac{B^{u_o} \delta A^{u_o} - A^{u_o} \delta B^{u_o}}{B^{u_o} \left(1 + \frac{\delta B^{u_o}}{B^{u_o}} \right)}$$

and using the fact that $\frac{1}{1+x} \approx 1-x$ when x is small, we have

$$\delta u_o = \frac{1}{B^{u_o} \left(1 + \frac{\delta B^{u_o}}{B^{u_o}} \right)} (B^{u_o} \delta A^{u_o} - A^{u_o} \delta B^{u_o}) \left(1 - \frac{\delta B^{u_o}}{B^{u_o}} \right);$$

neglecting second- and higher-order terms we have

$$\delta u_o \approx \frac{1}{B^{u_o} \left(1 + \frac{\delta B^{u_o}}{B^{u_o}} \right)} (B^{u_o} \delta A^{u_o} - A^{u_o} \delta B^{u_o}). \quad (14)$$

Expanding (14) and neglecting δC^2 term we have

$$\delta u_o = K_{u_o} \delta C, \quad (15)$$

where

$$K_{u_o} = \frac{\sum_{k=1}^3 (C_{1k} + C_{3k} - 2C_{1k}C_{3k})}{\sum_{l=1}^3 C_{3l}^2}.$$

Similarly, we have

$$\delta v_o = K_{v_o} \delta C, \quad (16)$$

where

$$K_{v_o} = \frac{\sum_{k=1}^3 (C_{2k} + C_{3k} - 2C_{2k}C_{3k})}{\sum_{l=1}^3 C_{3l}^2}.$$

Clearly, in this approximation, the error in image center ($\delta u_o, \delta v_o$) (see (15) and (16)) is proportional to the error in the camera calibration matrix. If δC is Gaussian (see (5)) so is δu_o and δv_o [21] (see Fig. 11).

4.2. Effect of Noise (δC) on Scaling Factors α_x, α_y

Let δC be the error associated with the camera calibration matrix due to the error in measurements. We know that the scaling factors, α_x, α_y , can be estimated from C from (7). If $\delta u_o, \delta v_o$ are the errors in the image center u_o, v_o then the scaling factors α_x, α_y with an erroneous camera calibration matrix $C + \delta C$ can be estimated as

$$\begin{aligned} \alpha_x + \delta \alpha_x &= \sqrt{\frac{\sum_{k=1}^3 (C_{1k} + \delta C)^2}{\sum_{l=1}^3 (C_{3l} + \delta C)^2} - (u_o - \delta u_o)^2} \\ \alpha_y + \delta \alpha_y &= \sqrt{\frac{\sum_{k=1}^3 (C_{2k} + \delta C)^2}{\sum_{l=1}^3 (C_{3l} + \delta C)^2} - (v_o - \delta v_o)^2}. \end{aligned} \quad (17)$$

Now, we concentrate on the scaling factor in the x direction, namely α_x . Equation (17) can be written as

$$\alpha_x + \delta \alpha_x = \sqrt{\frac{A^{\alpha_x} + \delta A^{\alpha_x}}{B^{\alpha_x} + \delta B^{\alpha_x}} - (D^{\alpha_x} + \delta D^{\alpha_x})}, \quad (18)$$

where

$$\begin{aligned} A^{\alpha_x} &= \sum_{k=1}^3 C_{1k}^2 \\ B^{\alpha_x} &= \sum_{l=1}^3 C_{3l}^2 \\ D^{\alpha_x} &= u_o^2 \end{aligned}$$

$$\begin{aligned}\delta A^{\alpha_x} &= 2\delta C \sum_{k=1}^3 C_{1k} + 3\delta C^2 \\ \delta B^{\alpha_x} &= 2\delta C \sum_{k=1}^3 C_{3k} + 3\delta C^2 \\ \delta D^{\alpha_x} &= 2u_o \delta u_o + \delta u_o^2.\end{aligned}$$

Using the approximation $(B^{\alpha_x} + \delta B^{\alpha_x})^{-1} = B^{\alpha_x-1}(1 - \delta B^{\alpha_x}/B^{\alpha_x})$, when $\delta B^{\alpha_x} \ll B^{\alpha_x}$, we have

$$\alpha_x + \delta\alpha_x = \sqrt{\frac{A^{\alpha_x}}{B^{\alpha_x}} - D^{\alpha_x} + \frac{\delta A^{\alpha_x}}{B^{\alpha_x}} - \frac{A^{\alpha_x} \delta B^{\alpha_x}}{B^{\alpha_x 2}} - \frac{\delta A^{\alpha_x} \delta B^{\alpha_x}}{B^{\alpha_x 2}} - \delta D^{\alpha_x}}.$$

Neglecting second-order terms and observing that $\alpha_x = \sqrt{\frac{A^{\alpha_x}}{B^{\alpha_x}} - D^{\alpha_x}}$ we have

$$\alpha_x + \delta\alpha_x = \sqrt{\alpha_x^2 + \frac{\delta A^{\alpha_x}}{B^{\alpha_x}} - \frac{A^{\alpha_x} \delta B^{\alpha_x}}{B^{\alpha_x 2}} - \delta D^{\alpha_x}},$$

squaring on both sides and neglecting higher-order ($\delta\alpha_x^2$) term we have

$$\begin{aligned}2\alpha_x \delta\alpha_x &= \frac{\delta A^{\alpha_x}}{B^{\alpha_x}} - \frac{A^{\alpha_x} \delta B^{\alpha_x}}{B^{\alpha_x 2}} - \delta D^{\alpha_x} \\ \delta\alpha_x &= K_{\alpha_x} \delta C,\end{aligned}\tag{19}$$

where

$$K_{\alpha_x} = \frac{\frac{\sum_{k=1}^3 C_{1k}}{\sum_{i=1}^3 C_{ii}^2} - \frac{\sum_{k=1}^3 C_{1k}^2 \sum_{m=1}^3 C_{3m}^2}{(\sum_{i=1}^3 C_{ii}^2)^2} - K_{u_o} u_o}{\alpha_x}.$$

Similarly, we have

$$\delta\alpha_y = K_{\alpha_y} \delta C,\tag{20}$$

where

$$K_{\alpha_y} = \frac{\frac{\sum_{k=1}^3 C_{2k}}{\sum_{i=1}^3 C_{ii}^2} - \frac{\sum_{k=1}^3 C_{2k}^2 \sum_{m=1}^3 C_{3m}^2}{(\sum_{i=1}^3 C_{ii}^2)^2} - K_{v_o} v_o}{\alpha_y}.$$

It can be seen from (19) and (20) that the errors in the scaling factors $\delta\alpha_x$ and $\delta\alpha_y$ are proportional to the error in the camera calibration matrix. Since δC is Gaussian (5), so is $\delta\alpha_x$ and $\delta\alpha_y$ [21] (see Fig. 12).

4.3. Effect of Noise (δC) on Translation (t_x, t_y, t_z)

The translation parameters in the x, y, z directions, represented by t_x, t_y, t_z , can be represented in terms of the camera calibration matrix C and the intrinsic parameters and are given by (8). If δC is the error in the camera calibration matrix then, this introduces an error in the translation parameters $\delta t_x, \delta t_y, \delta t_z$ (see Fig. 13).

4.3.1. Translation in the x and y Directions

Let

$$A^{tx} = \sum_{l=1}^3 C_{34}^2$$

$$\delta A^{tx} = 2\delta C \sum_{l=1}^3 C_{34} + 3\delta C^2,$$

then from (8) we have

$$t_x = \frac{\frac{C_{14}}{A^{tx}} - u_o \frac{C_{34}}{A^{tx}}}{\alpha_x}$$

and

$$t_x + \delta t_x = \frac{\frac{C_{14} + \delta C}{A^{tx} + \delta A^{tx}} - (u_o + \delta u_o) \frac{C_{34} + \delta C}{A^{tx} + \delta A^{tx}}}{\alpha_x + \delta \alpha_x}.$$

Assuming $\frac{\delta A^{tx}}{A^{tx}}$ and $\frac{\delta \alpha_x}{\alpha_x}$ to be small and using the relation $(1+x)^{-1} = 1-x$ and neglecting higher-order terms we have

$$t_x + \delta t_x = \frac{\frac{C_{14}}{A^{tx}} - u_o \frac{C_{34}}{A^{tx}}}{\alpha_x} + \frac{\frac{C_{14}}{A^{tx}} \left(\frac{\delta C}{C_{14}} - \frac{\delta \alpha_x}{\alpha_x} - \frac{\delta A^{tx}}{A^{tx}} \right) - u_o \frac{C_{34}}{A^{tx}} \left(\frac{\delta C}{C_{34}} - \frac{\delta A^{tx}}{A^{tx}} + \frac{\delta u_o}{u_o} - \frac{\delta \alpha_x}{\alpha_x} \right)}{\alpha_x}$$

or

$$\delta t_x = \frac{\frac{C_{14}}{A^{tx}} \left(\frac{\delta C}{C_{14}} - \frac{\delta u_o}{u_o} - \frac{\delta A^{tx}}{A^{tx}} \right) - u_o \frac{C_{34}}{A^{tx}} \left(\frac{\delta C}{C_{34}} - \frac{\delta A^{tx}}{A^{tx}} + \frac{\delta u_o}{u_o} - \frac{\delta \alpha_x}{\alpha_x} \right)}{\alpha_x} \quad (21)$$

$$\delta t_x = K_{t_x} \delta C, \quad (22)$$

where

$$K_{t_x} = \frac{\frac{C_{14}}{\sum_{l=1}^3 C_{34}^2} \left(\frac{1}{C_{14}} - \frac{K_{u_o}}{\alpha_x} - \frac{2 \sum_{l=1}^3 C_{34}}{\sum_{l=1}^3 C_{34}^2} \right) - \frac{u_o C_{34}}{\sum_{l=1}^3 C_{34}^2} \left(\frac{1}{C_{34}} - \frac{2 \sum_{l=1}^3 C_{34}}{\sum_{l=1}^3 C_{34}^2} + \frac{K_{u_o}}{u_o} - \frac{K_{\alpha_x}}{\alpha_x} \right)}{\alpha_x}.$$

Similarly one can show

$$\delta t_y = K_{t_y} \delta C, \quad (23)$$

where

$$K_{t_y} = \frac{\frac{C_{24}}{\sum_{l=1}^3 C_{34}^2} \left(\frac{1}{C_{24}} - \frac{K_{u_y}}{\alpha_y} - \frac{2 \sum_{l=1}^3 C_{34}}{\sum_{l=1}^3 C_{34}^2} \right) - \frac{u_y C_{34}}{\sum_{l=1}^3 C_{34}^2} \left(\frac{1}{C_{34}} - \frac{2 \sum_{l=1}^3 C_{34}}{\sum_{l=1}^3 C_{34}^2} + \frac{K_{u_y}}{u_y} - \frac{K_{\alpha_y}}{\alpha_y} \right)}{\alpha_y}.$$

4.3.2. Translation in the z (t_z) Direction

From (8) we have

$$t_z + \delta t_z = \frac{C_{34} + \delta C}{\sum_{l=1}^3 (C_{3l} + \delta C)^2} = \frac{C_{34} + \delta C}{A^{t_z} \delta A^{t_z}}, \quad (24)$$

where

$$\begin{aligned} A^{t_z} &= \sum_{l=1}^3 C_{3l} \\ \delta A^{t_z} &= 2\delta C \sum_{l=1}^3 C_{3l} + 3\delta C^2. \end{aligned}$$

Assuming $\frac{\delta A^{t_z}}{A^{t_z}}$ is small, we have

$$\delta t_z = \frac{C_{34} + \delta C}{A^{t_z} + \delta A^{t_z}} - \frac{C_{34}}{A^{t_z}} = \frac{C_{34}}{A^{t_z}} \left(1 + \frac{\delta C}{C_{34}} \right) \left(1 - \frac{\delta A^{t_z}}{A^{t_z}} \right) - \frac{C_{34}}{A^{t_z}}.$$

Neglecting higher-order term δC^2 , we have

$$\delta t_z = \frac{C_{34}}{A^{t_z}} \left(\frac{\delta C}{C_{34}} - \frac{\delta A^{t_z}}{A^{t_z}} \right) \quad (25)$$

$$= t_z \left(\frac{\delta C}{C_{34}} - \frac{\delta A^{t_z}}{A^{t_z}} \right) \quad (26)$$

$$= K_{t_z} \delta C. \quad (27)$$

where

$$K_{t_z} = t_z \left(\frac{1}{C_{34}} - \frac{2 \sum_{l=1}^3 C_{3l}}{\sum_{l=1}^3 C_{3l}^2} \right).$$

So, the errors in the translation parameters, δt_x , δt_y , and δt_z , are directly proportional to δC and it is clear that if δC has a Gaussian distribution (see (5)), so do the errors in the translation parameters [21].

4.4. Effect of Noise (δC) on the Rotation Parameters

The roll (ϕ), pitch (θ), and vergence (ξ) are shown in Fig. 2 and are given in (10). Using (10) we can write the roll as

$$\phi = \tan^{-1} \left(\frac{C_{21} - v_o C_{31} \alpha_x}{C_{11} - u_o C_{31} \alpha_y} \right)$$

$$\phi = \tan^{-1} \left(\frac{A^\phi \alpha_x}{B^\phi \alpha_y} \right),$$

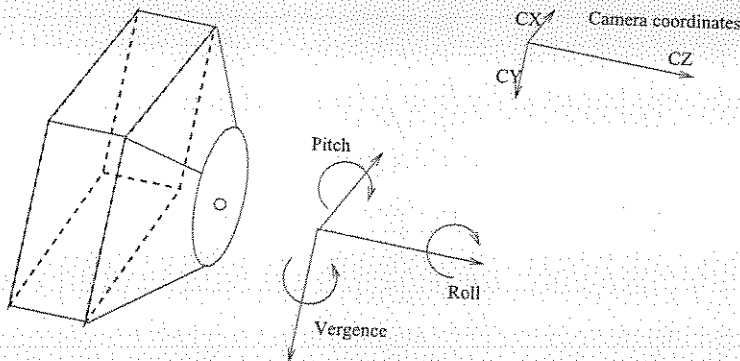


FIG. 2. Orientation angles—rotation about the camera x , y , z axes are referred to as pitch, vergence, and roll, respectively.

where

$$A^\phi = \frac{C_{21}}{\sum_{l=1}^3 C_{3l}^2} - v_o \frac{C_{31}}{\sum_{l=1}^3 C_{3l}^2}$$

$$B^\phi = \frac{C_{11}}{\sum_{l=1}^3 C_{3l}^2} - u_o \frac{C_{31}}{\sum_{l=1}^3 C_{3l}^2}.$$

If

$$\delta A^\phi = \delta C - 2C_{21}\delta C \frac{\sum_{l=1}^3 C_{3l}}{\sum_{l=1}^3 C_{3l}^2} - v_o C_{31} \left(\frac{\delta v_o}{v_o} + \frac{\delta C}{C_{31}} - 2\delta C \frac{\sum_{l=1}^3 C_{3l}}{\sum_{l=1}^3 C_{3l}^2} \right)$$

$$\delta B^\phi = \delta C - 2C_{11}\delta C \frac{\sum_{l=1}^3 C_{3l}}{\sum_{l=1}^3 C_{3l}^2} - u_o C_{31} \left(\frac{\delta u_o}{u_o} + \frac{\delta C}{C_{31}} - 2\delta C \frac{\sum_{l=1}^3 C_{3l}}{\sum_{l=1}^3 C_{3l}^2} \right),$$

then

$$\phi + \delta\phi = \tan^{-1} \left(\frac{A^\phi + \delta A^\phi}{B^\phi + \delta B^\phi} \frac{\alpha_x + \delta\alpha_x}{\alpha_y + \delta\alpha_y} \right).$$

Assuming $\frac{\delta B^\phi}{B^\phi}$ and $\frac{\delta\alpha_x}{\alpha_x}$ to be small and using the approximation $(1+x)^{-1} = 1-x$, we have

$$\phi + \delta\phi = \tan^{-1} \left(\frac{A^\phi}{B^\phi} \frac{\alpha_x}{\alpha_y} \left(1 + \frac{\delta A^\phi}{A^\phi} - \frac{\delta B^\phi}{B^\phi} + \frac{\delta\alpha_x}{\alpha_x} - \frac{\delta\alpha_y}{\alpha_y} \right) \right)$$

$$\tan(\phi + \delta\phi) = \tan\phi \left(1 + \frac{\delta A^\phi}{A^\phi} - \frac{\delta B^\phi}{B^\phi} + \frac{\delta\alpha_x}{\alpha_x} - \frac{\delta\alpha_y}{\alpha_y} \right).$$

Using the relationship $\tan\delta\phi \approx \delta\phi$ when $\delta\phi$ is small, we have

$$\frac{\tan\phi + \delta\phi}{1 - \tan\phi\delta\phi} = \tan\phi \left(1 + \frac{\delta A^\phi}{A^\phi} - \frac{\delta B^\phi}{B^\phi} + \frac{\delta\alpha_x}{\alpha_x} - \frac{\delta\alpha_y}{\alpha_y} \right)$$

$$\delta\phi = \frac{\tan\phi \left(\frac{\delta A^\phi}{A^\phi} - \frac{\delta B^\phi}{B^\phi} + \frac{\delta\alpha_x}{\alpha_x} - \frac{\delta\alpha_y}{\alpha_y} \right)}{1 + \tan^2\phi \left(1 + \frac{\delta A^\phi}{A^\phi} - \frac{\delta B^\phi}{B^\phi} + \frac{\delta\alpha_x}{\alpha_x} - \frac{\delta\alpha_y}{\alpha_y} \right)}$$

$$\begin{aligned}
 &= \frac{\tan \phi \left(\frac{\delta A^\phi}{A^\phi} - \frac{\delta B^\phi}{B^\phi} + \frac{\delta \alpha_x}{\alpha_x} - \frac{\delta \alpha_y}{\alpha_y} \right)}{\sec^2 \phi + \tan^2 \phi \left(\frac{\delta A^\phi}{A^\phi} - \frac{\delta B^\phi}{B^\phi} + \frac{\delta \alpha_x}{\alpha_x} - \frac{\delta \alpha_y}{\alpha_y} \right)} \\
 &= \frac{K_{\phi_o} \delta C}{\sec^2 \phi + K_{\phi_o} \delta C}, \tag{28}
 \end{aligned}$$

where

$$\begin{aligned}
 K_{\phi_o} = \tan \phi &\left(\left\{ 1 - 2C_{21} \frac{\sum_{l=1}^3 C_{3l}}{\sum_{l=1}^3 C_{3l}^2} - v_o C_{31} \left(\frac{K_{u_o}}{v_o} + \frac{1}{C_{31}} - 2 \frac{\sum_{l=1}^3 C_{3l}}{\sum_{l=1}^3 C_{3l}^2} \right) \right\} \right. \\
 &- \left. \left\{ 1 - 2C_{11} \frac{\sum_{l=1}^3 C_{3l}}{\sum_{l=1}^3 C_{3l}^2} - u_o C_{31} \left(\frac{K_{u_o}}{u_o} + \frac{1}{C_{31}} - 2 \frac{\sum_{l=1}^3 C_{3l}}{\sum_{l=1}^3 C_{3l}^2} \right) \right\} + \frac{K_{\alpha_x}}{\alpha_x} - \frac{K_{\alpha_y}}{\alpha_y} \right)
 \end{aligned}$$

$$K_{\phi_d} = K_{\phi_o} \tan \phi.$$

The orientation angle ϕ is affected in a manner more *complicated* than that of either of the other parameters (intrinsic and translation). It is not difficult to see that the other two orientation parameters, θ and ξ , will be related to the error δC in a more involved way because, as seen in (9), θ and ξ are dependent on ϕ . It is not immediately apparent whether $\delta\phi$, $\delta\theta$ and $\delta\xi$ have any particular distribution when δC is Gaussian, but simulation results (Section 5, Fig. 14) show that the error in the orientation parameters appear Gaussian when δC has Gaussian distribution.

5. EXPERIMENTAL RESULTS

Experiments were conducted to determine the error statistics of the camera calibration parameters due to error in determining the points in the image plane. A calibrated wedge (Fig. 1) with precisely marked points was used to estimate the camera calibration parameters. A sample scene as imaged by the Pulnix 6EX camera is shown in Fig. 1b, and the positions of the points have been marked manually as shown in Fig. 3. Marking these points manually

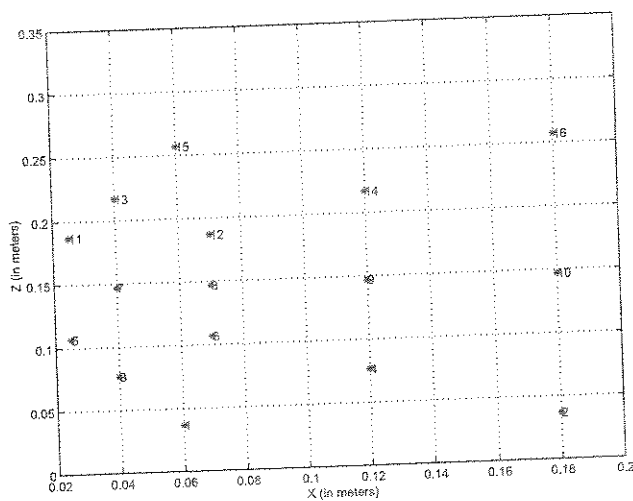


FIG. 3. The points on the plane B as marked on the structure. The units are in meters.

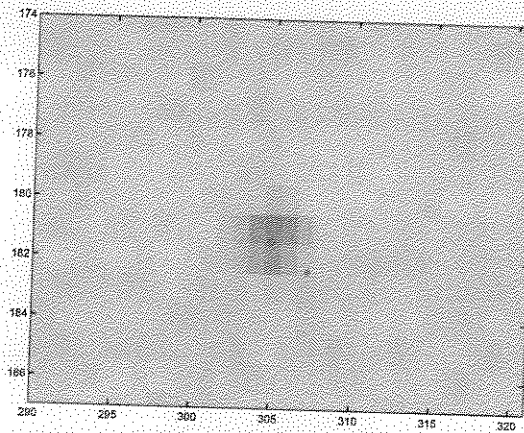


FIG. 4. The “*” denotes the approximate location of the image coordinate as determined manually and “o” determines the refined image coordinate using the method of moments.

is an error-prone process because the points need to be identified with a subpixel precision while what we can achieve at best, manually, is an accuracy to a pixel. Figure 4 shows the error in marking the points manually and that obtained by using the method of moments to refine feature point centroids to subpixel accuracy. The procedure to obtain subpixel accuracy is as follows:

- The lowest¹ intensity pixel within a 10×10 region of each manually selected point was located.
- The average background intensity, I_b , was computed from the intensity at the four corners of a square window about the center point.
- Average background intensity was subtracted from all pixels in the region and the weighted average coordinates were computed:

$$\bar{u} = \frac{\sum_i \sum_j i(I_{ij} - I_b)}{\sum_i \sum_j (I_{ij} - I_b)}$$

$$\bar{v} = \frac{\sum_i \sum_j j(I_{ij} - I_b)}{\sum_i \sum_j (I_{ij} - I_b)}.$$

The statistics of the error between the manual measurement and that obtained using the method of moments is shown in Fig. 5. One can observe that the plot is approximately Gaussian (mean = -0.186 and standard deviation 0.7087).

Before looking at the effect of noise, the points in the image plane were estimated to subpixel level accuracy using the method of moments. The camera calibration parameters determined using these values of $\{(u_i, v_i)\}_{i=1}^N$ are given in Table 1. These camera calibration parameters are accurate in the sense that there is no introduced error in the measured image points $\{(u_i, v_i)\}$; thus Table 1 gives the camera calibration parameters when the measurements have no additional noise component.

Next we look at the statistics of the camera parameters when noise with known statistics is introduced into the process of determining the feature point centroids $\{(u_i, v_i)\}$. We use Monte Carlo simulation methods [22] to determine the effect of noise. The experimental procedure is as follows.

¹ The calibration marks were black on white.

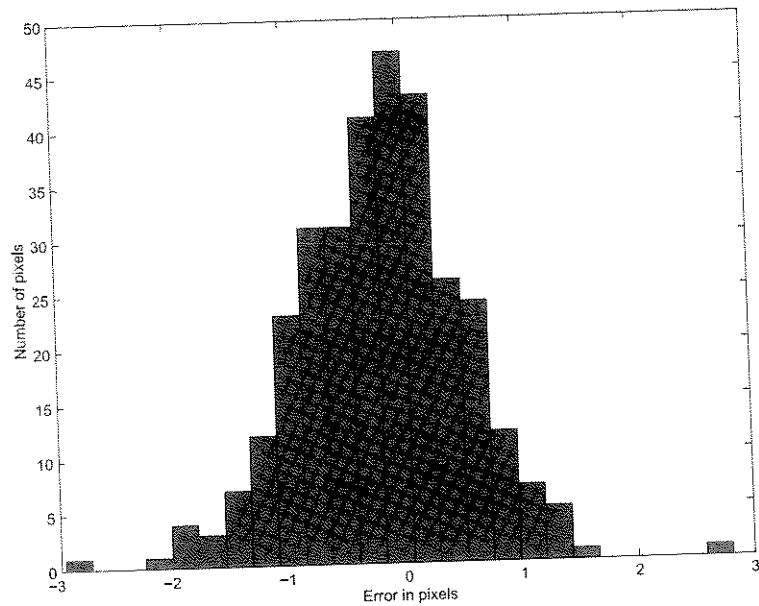


FIG. 5. Histogram of the error between the manual method and using the method of moments to mark the image points. Along the x axis is the error in pixels and along the y axis is the number of pixels.

Zero-mean Gaussian noise with different variance was added to the measured image points $\{(u_i, v_i)\}_{i=1}^N$, and these values were used to determine the camera calibration parameters. The different variances in the Gaussian noise corresponds to varying noise levels, which directly relates to the error made (in pixels) while measuring the calibration points in the image. We have studied the effect of noise that is Gaussian with standard deviation varying from 0.05 to 1 pixel. Experiments were carried out 2000 times for a given noise variance, and the statistics of the camera calibration parameters were estimated from these sample runs.

It can be observed from the simulations (Figs. 6–9f) that both the intrinsic and extrinsic parameters degrade with increasing noise levels. In addition it can be observed that an increase in noise variance increases the variability in the determined camera parameters *almost linearly* for all the camera calibration parameters. Furthermore, an increase in the noise variance introduces a bias in all the parameters, except in roll and pitch orientations (see Fig. 8e) and translation along the z axis (see Fig. 9e). Figures 6a–6d show the image center for all the 2000 runs for various noise levels. It is seen that the cluster of image centers

TABLE I
The Camera Parameters (Extrinsic) Determined from the Feature
Centroid Estimates Obtained Using the Method of Moments

Principle point (u_o, v_o)			(379.36, 131.47)		
Scale factor (α_x, α_y)			(949.21, 471.18)		
Rotation (°)			Translation (m)		
Roll	Pitch	Vergence	x	y	z
No noise	1.50	-88.78	-44.86	-0.0477	0.1703
					0.6783

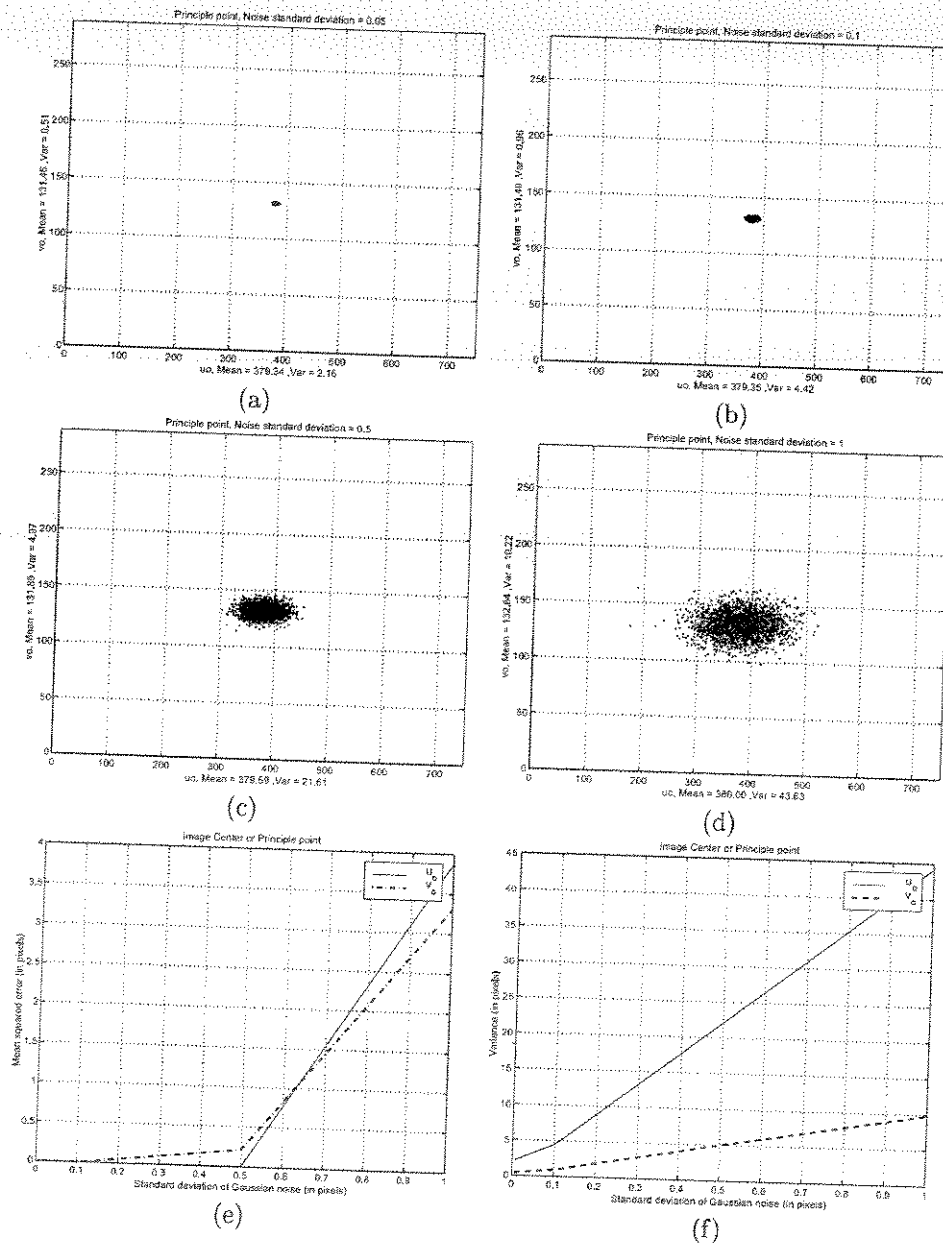


FIG. 6. Variation of image center (u_o , v_o) with varying noise levels: (a) 0.05, (b) 0.1, (c) 0.5, and (d) 1 pixel standard deviation. (e) Mean-squared error of the image center as a function of noise, and (f) the variance of the determined image center as a function of noise level.

shifts with increasing noise. Figure 6d compares the mean-squared error of the image center for different noise levels, and Fig. 6e shows the mean-squared error in estimating the image center with varying noise levels. It can be observed that there is a significant shift from the *real* image center when the noise standard deviation is greater than 0.5 pixels. This suggests that the image point locations need to necessarily be determined to a subpixel accuracy. Figure 6f is an indication of the size of the cluster and shows that the variation in the determined image centers increases when the noise levels increases.

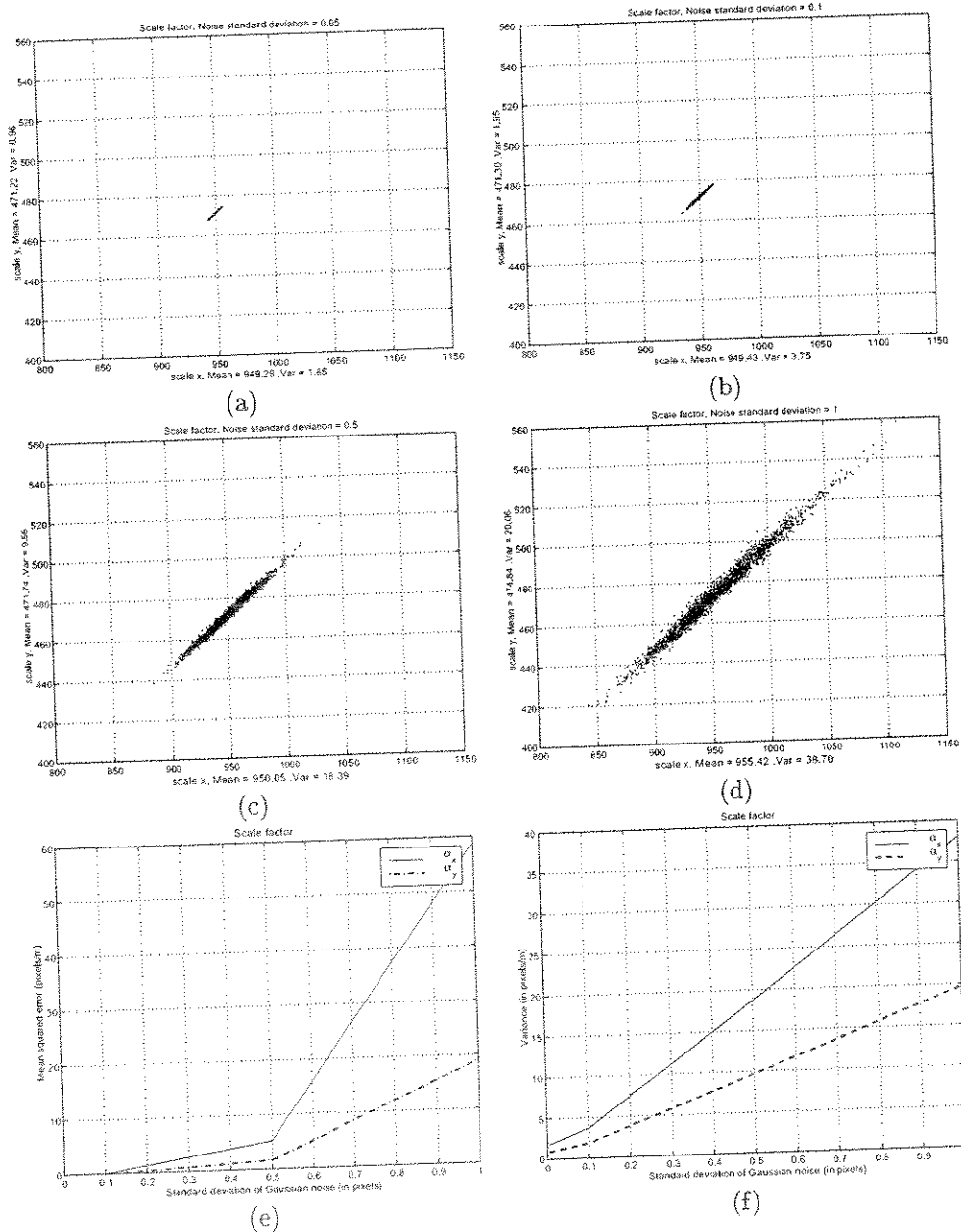


FIG. 7. The variation of the intrinsic parameters scale factor (α_x, α_y) with varying noise levels of (a) 0.05, (b) 0.1, (c) 0.5, and (d) 1 pixel, respectively; (e) and (f) show the mean-squared error and variance, respectively, of the scale factors as a function of noise levels.

Figures 7a–7f capture the effect of noise on the scale factor. Figures 7a–7d shows the variation of these parameters along both x and y directions for noise standard deviations of 0.05, 0.1, 0.5, and 1.0 pixel. The estimates of the scale factor degrade with increase in noise level. It is interesting to note that the noise affects the scale factors in a *similar direction*; namely, if the scale factor along x is less than the mean value, then so is the scale factor in the y direction.

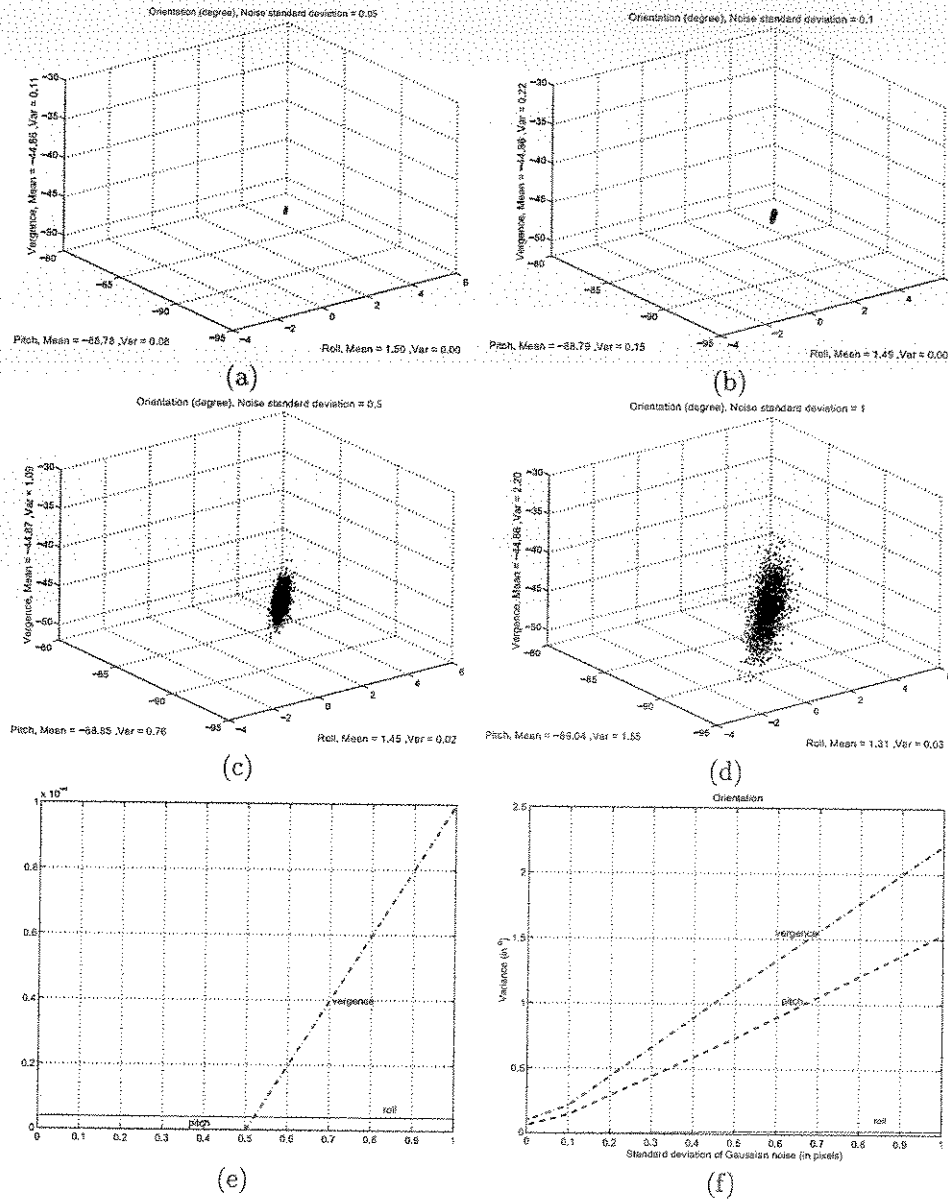


FIG. 8. (a)–(d) shows the variation of the extrinsic parameters (orientation, roll, pitch, and vergence in degrees) with varying noise levels. (e) shows the mean-squared error in the orientation parameters with varying noise levels. and (f) shows the variance as a function of noise variance.

Figures 8a–8d and 9a–9d depict the variation of the orientation and translation parameters as a function of noise (standard deviation 0.05, 0.1, 0.5, and 1.0 pixels). These are 3D plots with each direction being denoted by roll, pitch, and vergence (rotations about the z , x , and y axes, respectively) and x , y , and z translations (Fig. 9). It can be observed from Fig. 8e that not all orientation parameters are affected to the same extent by noise. The vergence angle seems to be less robust to noise than the roll or the pitch parameters. Observe that there is a small variation in the orientation parameters at a noise level of 0.05 pixels but even this small variation can significantly alter the image, thus rendering the image useless for

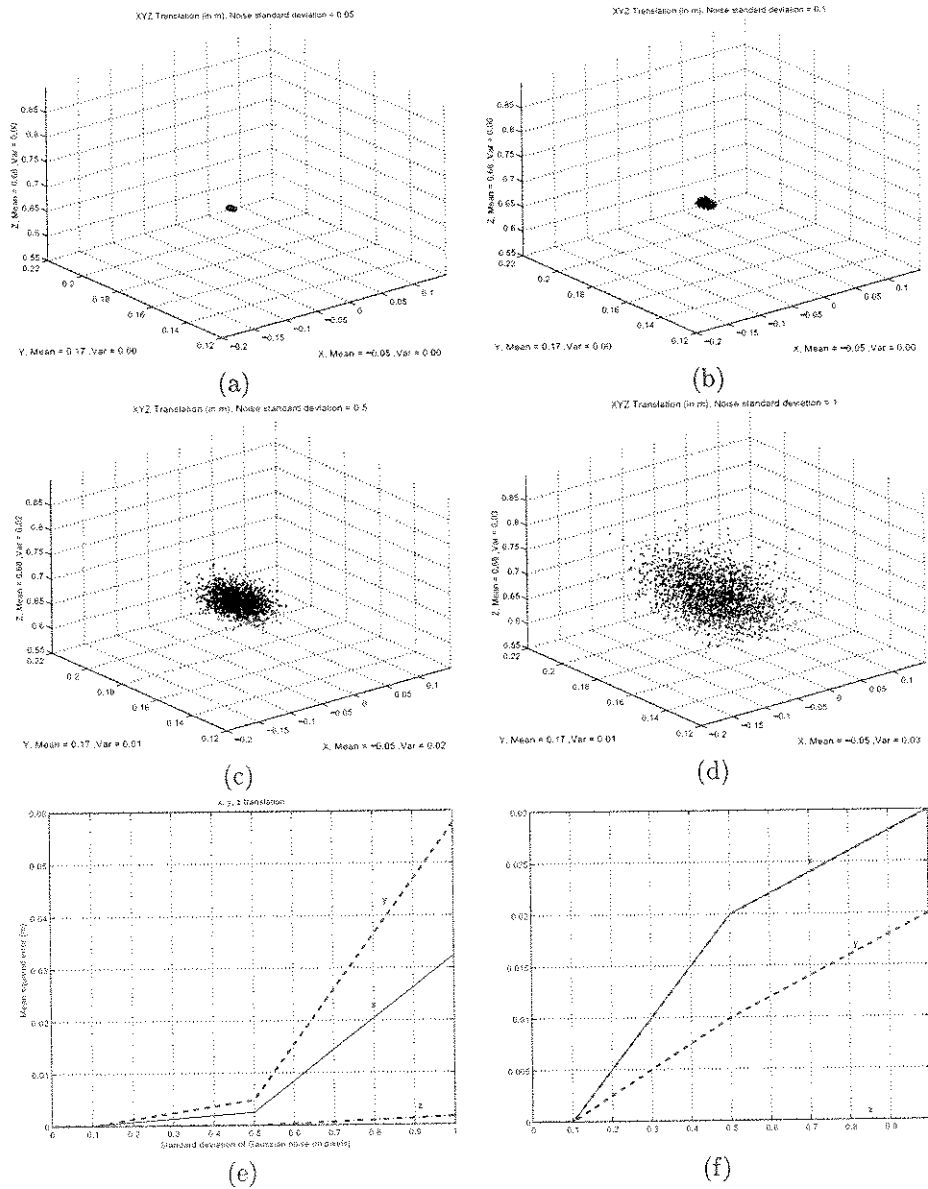


FIG. 9. (a)-(d) shows the variation of the extrinsic parameters (translation in the x , y , and z directions) with varying noise levels. (e) shows the mean-squared error of the translation parameters with varying noise levels, and (f) show a plot of the variance of these parameters as a function of noise.

some applications (for example, in stereo vision where one is looking for images satisfying epipolar line constraint). To appreciate this, consider an error of 1° in one of the orientation parameters, and if the focal length of the camera is 8 mm and the size of the pixel is $11 \mu\text{m}$, then a 1° error results in a shift of 0.16 mm ($\tan(1^\circ) \times 8$). This translates to approximately 14 ($0.16 \times 10^{-3} / 11 \times 10^{-6}$) pixels across the line, which in most stereo vision applications is unacceptable.

Figures 11–14 show the distribution of the error in the camera calibration parameters when the error in the camera calibration matrix is Gaussian (for the purpose of illustration

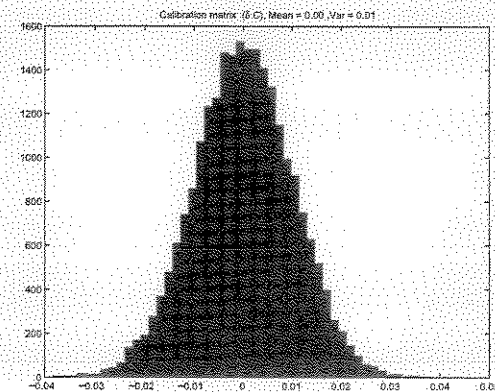


FIG. 10. Histogram plot of error in the camera calibration matrix δC .

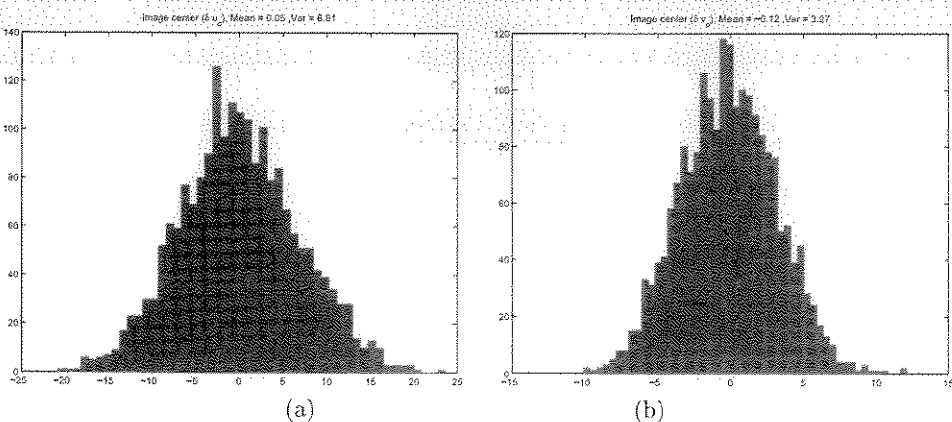


FIG. 11. Histogram plot of error in image center: (a) δu_0 and (b) δv_0 .

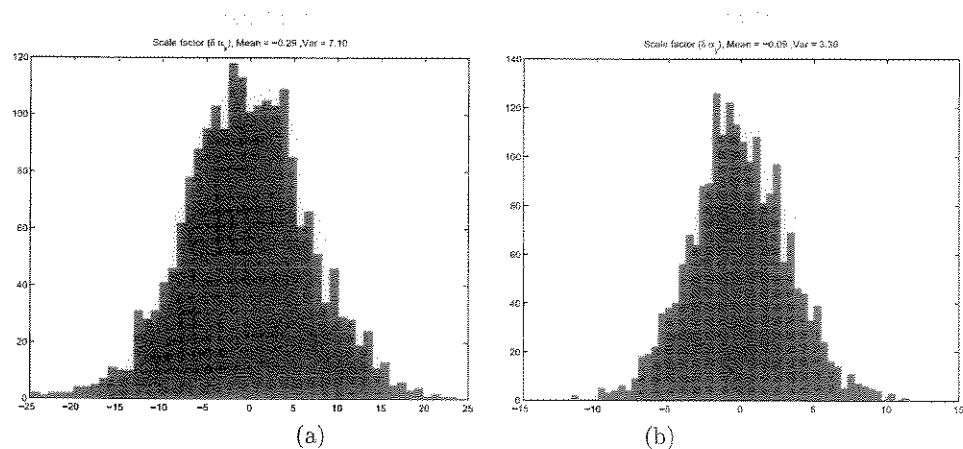


FIG. 12. Histogram plot of error in scaling factor: (a) $\delta \alpha_3$ and (b) $\delta \alpha_{11}$.

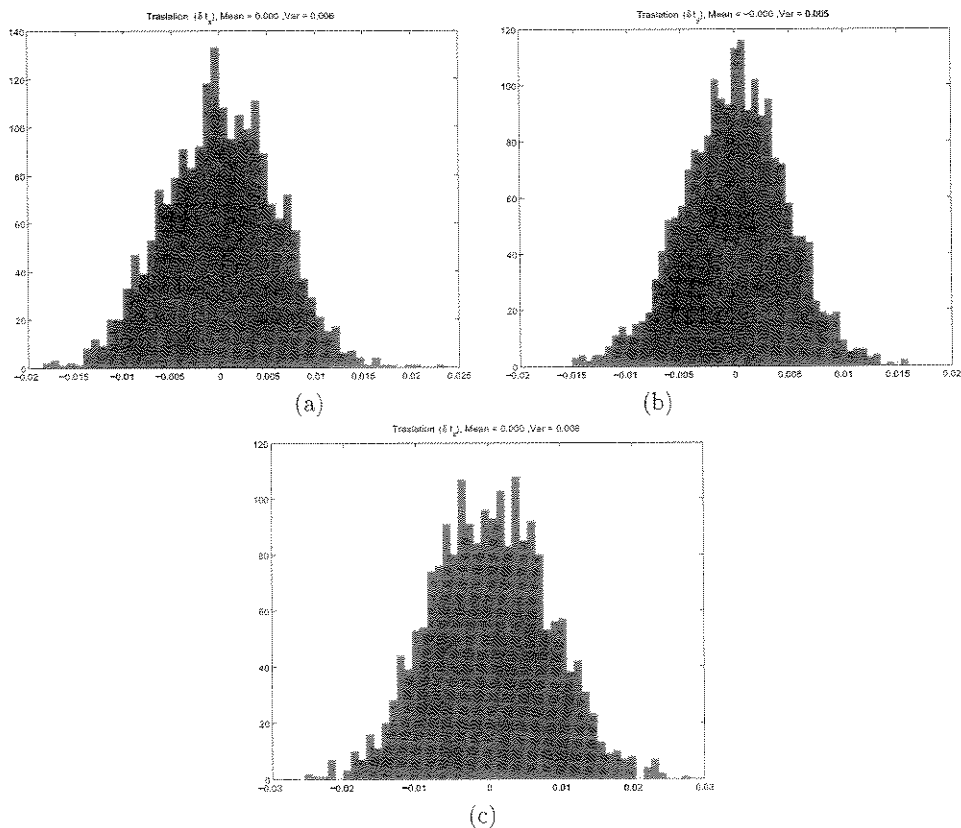


FIG. 13. Histogram plot of error in translation: (a) δt_x , (b) δt_y , and (c) δt_z .

we have assumed a Gaussian of mean zero and variance 0.01, Fig. 10). It can be observed that all the errors in the camera calibration parameters have a Gaussian-like distribution when the error in the camera calibration matrix (δC) is Gaussian due to error in the measurement of (u, v) . Further, these experimental results closely support the results derived in Section 4. Table 2 captures the appropriateness of the approximations made in Section 4 and relates them to the experimental results (Figs. 11–14). Note that because of the way $\delta\phi$ and δC

TABLE 2
Comparing Theoretical (Section 4) and Experimental Results

Parameter	Mean		Variance	
	Experimental	Theoretical	Experimental	Theoretical
δu_o	0.05	0	6.81	7.61
δv_o	-0.12	0	3.27	4.47
$\delta \alpha_x$	-0.29	0	7.10	7.95
$\delta \alpha_y$	-0.09	0	3.36	3.83
δt_x	0	0	0.006	0.005
δt_y	0	0	0.005	0.004
δt_z	0	0	0.008	0.004
ϕ	0.01	—	0.4	—

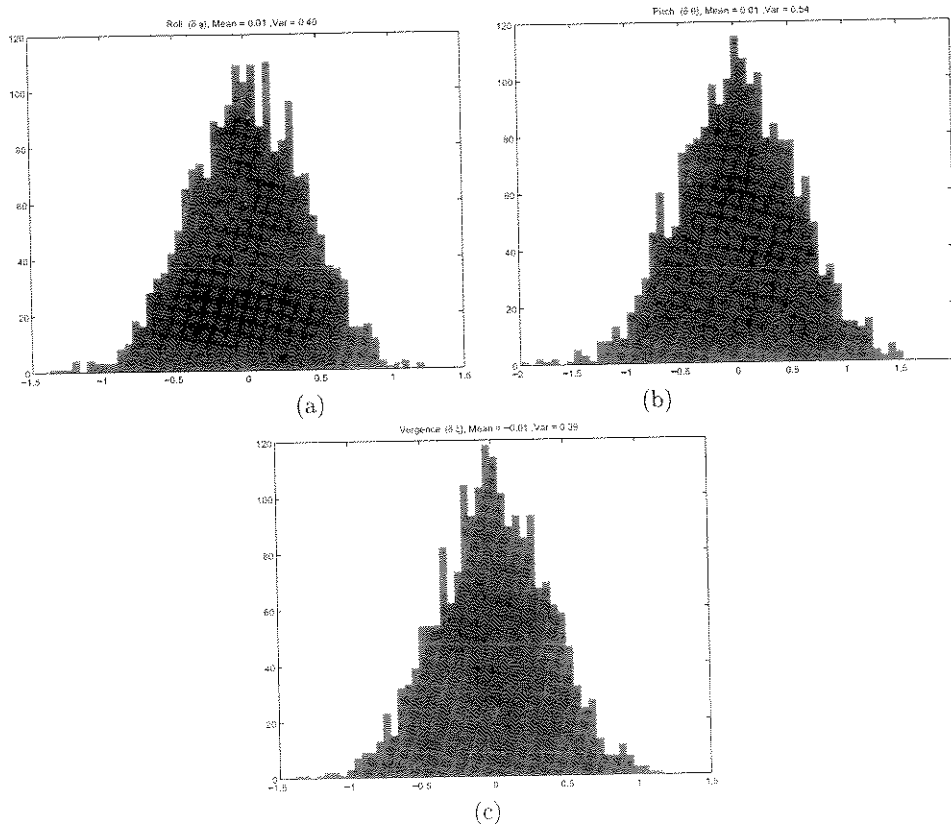


FIG. 14. Histogram plot of error in translation: (a) $\delta\phi$, (b) $\delta\theta$, and (c) δg .

are related, the mean and variance of $\delta\phi$ cannot be estimated theoretically, unlike other parameters.

6. CONCLUSIONS

The usual procedure for determining the camera calibration parameters is to first determine the camera calibration matrix using the correspondence between the points in 3D space and their projection onto the 2D image plane of the camera and then decompose the camera calibration matrix to determine the camera calibration parameters. In this paper, we follow this procedure to determine the camera calibration parameters and show how the various camera calibration parameters are affected by noisy image measurements. This analysis has practical application, especially for a field engineer, and can be used to justify the accuracy with which the measurements need to be made so that the camera calibration parameters are within an acceptable error tolerance. As expected, the Monte Carlo simulations show that the camera calibration parameters degrade with increase in noise. This fact is reinforced by theory. For example, through (16) we have established that the error in the image center is Gaussian and is proportional to the error in the measurement, which implies that an increase in error contributes to the increase in the error in estimation of the calibration parameters. We observe that the orientation parameters are more complexly involved and hence more prone to noise in measurements than the other parameters (image center, scaling factor, and translation). Simulations show that, within the orientation parameters, the degradation is

more forgiving in the case of some parameters (pitch, roll) than others (vergence) (Figs. 8e and 8f).

APPENDIX A

Decomposition of Camera Calibration Matrix C

The camera calibration matrix \mathbf{C} captures explicitly:

1. World coordinate to camera coordinate transformation:

$$\begin{bmatrix} {}^c x \\ {}^c y \\ {}^c z \end{bmatrix} = \underbrace{\begin{bmatrix} r_{11} & r_{12} & r_{13} \\ r_{21} & r_{22} & r_{23} \\ r_{31} & r_{32} & r_{33} \end{bmatrix}}_{\mathbf{R}} \begin{bmatrix} x \\ y \\ z \end{bmatrix} + \underbrace{\begin{bmatrix} t_x \\ t_y \\ t_z \end{bmatrix}}_{\underline{t}}. \quad (29)$$

The world coordinates are converted to the camera 3D coordinate system $[{}^c x \ {}^c y \ {}^c z]^T$ by the rotation matrix \mathbf{R} and the translation vector \underline{t} .

2. Perspective transformation: The camera coordinate system is projected onto the image plane $[u' \ v']^T$ by the perspective transformation. If f is the focal length of the camera that is used to image then

$$\begin{bmatrix} u' \\ v' \end{bmatrix} = \begin{bmatrix} \frac{f}{f - {}^c z} & 0 \\ 0 & \frac{f}{f - {}^c z} \end{bmatrix} \begin{bmatrix} {}^c x \\ {}^c y \end{bmatrix}. \quad (30)$$

3. Scaling and offset:

$$\begin{bmatrix} u \\ v \end{bmatrix} = \begin{bmatrix} \alpha_x & 0 \\ 0 & \alpha_y \end{bmatrix} \begin{bmatrix} u' \\ v' \end{bmatrix} + \begin{bmatrix} u_o \\ v_o \end{bmatrix}, \quad (31)$$

where α_x and α_y are the scaling (units of pixels/m) in the x and the y directions and u_o , v_o are the offset (units of pixels) in the image. The scaling is caused not only because of the differences in the frequency of operation of the camera and the digitizer but also due to the size of the camera's photosite. The offset is caused because of the origin shift (see Fig. 15).

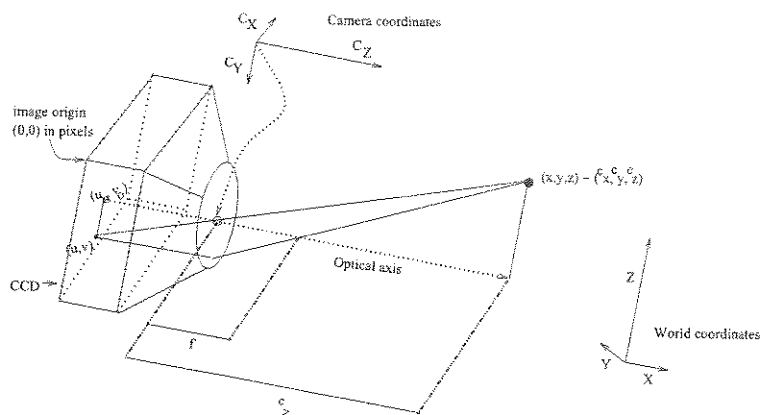


FIG. 15. Origin offset—image center and camera center. Image is projected onto the place $z = -f$ by an ideal thin lens at $z = 0$.

APPENDIX B

Given the pdf of X and Y , find the pdf of $Z = b^{-1}(X - aY)$

Given constants a and b and random variables X and Y , which are independent and Gaussian distributed with mean 0 and variance σ_x^2 and σ_y^2 , respectively, we need to find the probability density function of the random variable Z . Letting $Q = aY$, we know that if Y has the pdf

$$f_Y(y) = \frac{1}{\sqrt{2\pi\sigma_y^2}} \exp^{-\frac{y^2}{2\sigma_y^2}},$$

then Q will have [21]

$$f_Q(q) = \frac{1}{\sqrt{2\pi a^2\sigma_y^2}} \exp^{-\frac{q^2}{2a^2\sigma_y^2}}.$$

Let $K = (X - Q)$; since we know that X and Y are independent, so are X and Q . Now, we can write the pdf of K as a convolution

$$\begin{aligned} f_K(k) &= \int_{-\infty}^{\infty} f_X(k+q) f_Q(q) dq \\ &= \int_{-\infty}^{\infty} \frac{1}{\sqrt{2\pi\sigma_x^2}} \exp^{-\frac{(k+q)^2}{2\sigma_x^2}} \frac{1}{\sqrt{2\pi a^2\sigma_y^2}} \exp^{-\frac{q^2}{2a^2\sigma_y^2}} dq \\ &= \frac{1}{\sqrt{2\pi\sigma_x^2}} \frac{1}{\sqrt{2\pi a^2\sigma_y^2}} \int_{-\infty}^{\infty} \exp^{-\left\{ \frac{(k+q)^2}{2\sigma_x^2} + \frac{q^2}{2a^2\sigma_y^2} \right\}} dq \\ &= \frac{1}{\sqrt{2\pi\sigma_x^2}} \frac{1}{\sqrt{2\pi a^2\sigma_y^2}} \int_{-\infty}^{\infty} \exp^{-\left\{ \frac{\frac{(k+q)^2}{2\sigma_x^2} + \frac{q^2}{2a^2\sigma_y^2} - \frac{k^2\sigma_x^4\sigma_y^4}{2\sigma_x^2\sigma_y^2 + \sigma_x^2\sigma_y^4}}{2\sigma_x^2\sigma_y^2} \right\}} dq \\ &= \frac{1}{\sqrt{2\pi\sigma_x^2}} \frac{1}{\sqrt{2\pi a^2\sigma_y^2}} \int_{-\infty}^{\infty} \exp^{-\left(\frac{\frac{(k+q)^2\sigma_x^4}{2\sigma_x^2\sigma_y^2} - \frac{q^2\sigma_x^4\sigma_y^4}{2\sigma_x^2\sigma_y^2 + \sigma_x^2\sigma_y^4}}{2\sigma_x^2\sigma_y^2} \right)} dq. \quad (32) \end{aligned}$$

We know from the definition of a pdf that

$$\frac{1}{\sqrt{2\pi \frac{\sigma_x^2\sigma_y^4 + \sigma_y^2\sigma_x^4}{\sigma_x^2\sigma_y^2 + \sigma_y^2}}} \int_{-\infty}^{\infty} \exp^{-\frac{\left(q - \frac{k\sigma_x^2\sigma_y^2}{\sigma_x^2\sigma_y^2 + \sigma_y^2} \right)^2}{\frac{\sigma_x^2\sigma_y^4 + \sigma_y^2\sigma_x^4}{\sigma_x^2\sigma_y^2 + \sigma_y^2}}} dq = 1. \quad (33)$$

Now, we can write (32) as

$$f_K(k) = \sqrt{2\pi} \frac{\sigma_x^2 a^2 \sigma_y^2}{a^2 \sigma_y^2 + \sigma_x^2} \frac{1}{\sqrt{2\pi \sigma_x^2}} \frac{1}{\sqrt{2\pi a^2 \sigma_y^2}} \exp^{-\left(\frac{k^2 a^2 \sigma_y^4}{2\sigma_x^2 a^2 \sigma_y^2}\right)}, \quad (34)$$

which can be simplified to

$$f_K(k) = \frac{1}{\sqrt{2\pi (\sigma_x^2 + a^2 \sigma_y^2)}} \exp^{-\left(\frac{k^2}{2\sigma_x^2 + a^2 \sigma_y^2}\right)},$$

which implies that the random variable K is a Gaussian random variable with mean 0 and variance $(\sigma_x^2 + a^2 \sigma_y^2)$. Since $Z = b^{-1}K$, we know that the random variable Z too has Gaussian distribution with mean 0 and variance $b^{-2}(\sigma_x^2 + a^2 \sigma_y^2)$; that is,

$$f_Z(z) = \frac{1}{\sqrt{2\pi b^{-2}(\sigma_x^2 + a^2 \sigma_y^2)}} \exp^{-\left(\frac{z^2}{2b^{-2}(\sigma_x^2 + a^2 \sigma_y^2)}\right)}.$$

ACKNOWLEDGMENTS

Thanks are due to Dr Kim Ng, who kindly loaned the calibration target (Fig. 1), which was developed for the SHAPE system at the Monash University, Australia. The authors also thank the Automation Group for the various simulating discussions and for creating a great working environment.

REFERENCES

1. O. D. Faugeras and G. Toscani, The calibration problem for stereo, in *IEEE Computer Vision and Pattern Recognition*, pp. 15–20, 1986.
2. W. Y. Zhao and N. Nandakumar, Effects of camera alignment errors on stereoscopic depth estimates, *Pattern Recognit.* **29**, 1996, 2115–2126.
3. A. L. Abbott and N. Ahuja, Active stereo: Integrating disparity, vergence, focus, aperture, and calibration for surface estimation, *IEEE Trans. Pattern Anal. Mach. Intell.* **15**, 1993, 1007–1029.
4. G. Q. Wei and S. D. Ma, Implicit and explicit camera calibration—Theory and experiments, *IEEE Trans. Pattern Anal. Mach. Intell.* **16**, 1994, 469–480.
5. B. Caprile and V. Torre, Using vanishing points for camera calibration, *Internat. J. Comput. Vision* **4**, 1990, 127–140.
6. C. Chatterjee and V. Rowchowdhury, Efficient and robust methods of accurate camera calibration, in *IEEE Computer Vision and Pattern Recognition*, pp. 664–665, 1993.
7. C. C. Wang, A low-cost calibration method for automated optical mensuration using a video camera, *Mach. Vision Appl.* **7**, 1994, 259–266.
8. W. I. Grosky and L. A. Tamburino, A unified approach to the linear camera calibration problem, *IEEE Trans. Pattern Anal. Mach. Intell.* **12**, 1990, 663–671.
9. I. E. Sutherland, Three-dimensional data input by tablet, *Proc. IEEE* **62**, 1974, 453–461.
10. I. Sobel, On calibrating computer controlled cameras for perceiving 3-D scenes, *Artif. Intell. An Internat. J.* **5**, 1974, 85–198.
11. R. M. Haralick and L. G. Shapiro, *Computer and Robot Vision*, Addison-Wesley, Reading, MA, 1993.
12. J. L. Crowley, P. Bobet, and C. Schmid, Auto-calibration by direct observation of objects, *Image Vision Comput.* **11**, 1993, 67–81.

13. Q. T. Luong and O. Faugeras, Self-calibration of a stereo rig from unknown camera motions and point correspondences, Technical Report 2014, INRIA, France, 1993.
14. R. Horaud and G. Csurka, Self-calibration and Euclidean reconstruction using motions of a stereo rig, in *International Conference on Computer Vision, Bombay, India*, January 1998.
15. R. Y. Tsai, A versatile camera calibration technique for high accuracy 3-D machine vision metrology using off-the-shelf TV cameras and lenses, *IEEE Trans. Robot. Autom.* **3**, 1987, 323–344.
16. R. Kumar and A. R. Hanson, Robust estimation of camera location and orientation from noisy data having outliers, in *Workshop in Interpretation of 3D Scenes*, pp. 52–60, 1989.
17. R. Kumar and A. R. Hanson, Robust methods for estimating pose and sensitivity analysis, *CVGIP: Image Understand.* **60**, 1994, 313–342.
18. J. Z. C. Lai, On the sensitivity of camera calibration, *Image Vision Comput.* **11**, 1993, 656–664.
19. P. I. Corke, *Visual Control of Robots*, Research Studies Press, Taunton, UK, 1996.
20. S. Ganapathy, Decomposition of transformation matrices for robot vision, *Pattern Recognit. Lett.* **2**, 1984, 401–412.
21. A. Papoulis, *Probability, Random Variables, and Stochastic Processes*, McGraw-Hill, New York, 1991.
22. J. M. Hammersley and D. C. Handscomb, *Monte Carlo Methods*, Methuen, London, 1964.

